THE FASEB JOURNAL • RESEARCH • www.fasebj.org

Understanding the coupling between DNA damage detection and UvrA's ATPase using bulk and single molecule kinetics

Jamie T. Barnett and Neil M. Kad[1]
School of Biological Sciences, University of Kent, Canterbury, United Kingdom

ABSTRACT: Nucleotide excision repair (NER) protects cells against diverse types of DNA damage, principally UV irradiation. In *Escherichia coli*, damage is recognized by 2 key enzymes: UvrA and UvrB. Despite extensive investigation, the role of UvrA's 2 ATPase domains in NER remains elusive. Combining single-molecule fluorescence microscopy and classic biochemical methods, we have investigated the role of nucleotide binding in UvrA's kinetic cycle. Measurement of UvrA's steady-state ATPase activity shows it is stimulated upon binding DNA (k_{cat} 0.71–1.07/s). Despite UvrA's ability to discriminate damage, we find UV-damaged DNA does not alter the steady-state ATPase. To understand how damage affects UvrA, we studied its binding to DNA under various nucleotide conditions at the single molecule level. We have found that both UV damage and nucleotide cofactors affect the attached lifetime of UvrA. In the presence of ATP and UV damage, the lifetime is significantly greater compared with undamaged DNA. To reconcile these observations, we suggest that UvrA uses negative cooperativity between its ATPase sites that is gated by damage recognition. Only in the presence of damage is the second site activated, most likely in a sequential manner.—Barnett, J. T., Kad, N. M. Understanding the coupling between DNA damage detection and UvrA's ATPase using bulk and single molecule kinetics. FASEB J. 33, 000–000 (2019). www.fasebj.org

KEY WORDS: cooperativity · fluorescence imaging · DNA repair · DNA tightropes

Genomic DNA is constantly damaged by both exogenous and endogenous sources and must be repaired efficiently to maintain genome integrity. Nucleotide excision repair (NER) is an evolutionarily conserved DNA repair mechanism across all kingdoms of life. NER primarily repairs bulky lesions, including UV-induced damage, such as cyclobutane pyrimidine dimers and 6–4 photoproducts. However, NER also acts promiscuously to recognize and repair myriad lesion types (1). The classic description of NER involves the processing of the lesion by multiple enzymes and requires detection, incision, and repair resynthesis (2). Damage verification requires UvrA (a homodimer that is referred to as UvrA here for clarity) to locate damage with UvrB. Upon location of damage, UvrA is ejected from the UvrAB "preincision" complex, leaving UvrB alone on DNA. UvrC is then recruited to perform 2 DNA incisions on either side of the lesion on the same strand. Subsequently, UvrD and DNA polymerase I carry out downstream damaged oligonucleotide removal and repair resynthesis (3, 4). Finally, DNA ligase seals the remaining nick in the DNA backbone.

Successful lesion excision in *Escherichia coli* requires ATP (3, 5–7). Analysis of UvrA's sequence reveals 2 type A Walker motif sites, one at residues 31–45 (N-terminal site) and one at residues 640–654 (C-terminal site) (8). In the 3-dimensional structure of dimeric UvrA, the N-terminal ATPase domain of 1 UvrA is close to the C-terminal ATPase site of the other. Furthermore, all 4 are positioned beneath the DNA binding cleft that runs across the face of the protein (9, 10). The role of UvrA's ATPase activity is uncertain but has been linked to dimer formation and lesion searching (5, 11, 12). Previous studies that mutated catalytic lysine residues in each ATPase site observed a drastic loss of overall ATPase activity (13). Such mutational studies have indicated a role for ATPase in loading UvrB onto DNA (13, 14). Because many of these studies conflict in their outcomes, a clearly defined ATPase mechanism and definition of its role in UvrA's function is needed.

UvrA's ATPase sites are thought to have distinct roles (13, 15, 16); the C-terminal site discriminates DNA damage, and the N-terminal site is implicated in UvrA dimer formation and UvrB binding (17, 18). Using the *in vitro*

ABBREVIATIONS: ATPγS, adenosine 5′-O-(3-thio)triphosphate; NER, nucleotide excision repair; $UvrA_{WT}$, UvrA wild-type

[1] Correspondence: School of Biological Sciences, University of Kent, CT2 7NH Canterbury, United Kingdom. E-mail: n.kad@kent.ac.uk

doi: 10.1096/fj.201800899R
This article includes supplemental data. Please visit *http://www.fasebj.org* to obtain this information.

DNA tightrope assay in conjunction with mScarlet-labeled *E. coli* UvrA (19), we have investigated, at the single-molecule level, how different nucleotide cofactors affect UvrA's interaction with DNA. UvrA was observed to perform a 3-dimensional search on DNA, with a lifetime altered by the nucleotide condition, and the presence of UV damage. The rate-limiting step for ATP turnover occurs on DNA, and the presence of damage alters UvrA's DNA bound lifetime but not its steady-state ATPase rate. This paradox is resolved if UvrA sequentially hydrolyzes ATP in its 2 sites, suggesting that UvrA has a negatively cooperative ATPase that is tightly coupled to damage recognition.

MATERIALS AND METHODS

Unless stated otherwise, all chemicals were purchased from Thermo Fisher Scientific (Waltham, MA, USA), and DNA oligonucleotides were from MilliporeSigma (Burlington, MA, USA). All *in vitro* experiments were carried out at room temperature in ABC buffer [50 mM Tris–HCl (pH 7.5), 50 mM KCl, 10 mM $MgCl_2$, and 10 mM DTT].

Protein expression and purification

The gene for *E. coli* UvrA, obtained from National Bioresource Project (NIG, Kyoto, Japan), was engineered onto a C-terminal mScarlet fluorescent protein separated *via* a flexible linker (20). Further C-terminal to mScarlet, we placed a His tag for purification and induced expression of this pET21a construct overnight at 18°C using isopropyl β-D-1-thiogalactopyranoside. Purification was performed using nickel affinity followed by heparin chromatography (GE Healthcare, Chicago, IL, USA). To avoid protein precipitation, we kept KCl concentrations >200 mM. Once purified, the UvrA concentration was determined using mScarlet's extinction coefficient ($M^{-1}cm^{-1}$) at 569 nm and stored in 50% glycerol 50 mM Tris (pH 7.5), 500 mM KCl, 0.1 mM EDTA, and 10 mM DTT at −20°C (18).

Complementation assays

To investigate whether our UvrA-mScarlet construct can rescue UvrA wild-type ($UvrA_{WT}$) knockout cells, we performed *in vivo* UV complementation assays. $UvrA_{WT}$ knockout (Keio) cells were obtained from the National Bioresource Project (NIG) and transformed with UvrA-mScarlet or empty mScarlet vector. Previously, we have shown $UvrA_{WT}$ knockout cells complemented with ectopically expressed $UvrA_{WT}$ survive UV irradiation at 5 J/m^2 (21). Transformed cells were grown in Luria-Bertani medium with 25 μg/ml chloramphenicol to OD600 of 0.5. Five microliters of undiluted and three 10-fold serial dilutions were plated on Luria-Bertani agar and subjected to either no UV or 5 J/m^2 UV (254 nm) irradiation and incubated overnight at 37°C in the dark. $UvrA_{WT}$ and UvrA-mScarlet fully restored UV survival compared with $UvrA_{WT}$ knockout and $UvrA_{WT}$ knockout cells ectopically expressing mScarlet alone.

NADH-linked ATPase assay

ABC buffer supplemented with 0.5 mM phosphoenol pyruvate solution was stored at −20°C; 1 mM DTT was added upon thawing. The phosphoenol pyruvate solution with DTT was blanked at 340 nm in a spectrophotometer, and then 10 μl of pyruvate kinase (600–1000 U/ml) and lactate dehydrogenase (900–1400 U/ml, premixed stock from MilliporeSigma) per 500 μl reaction were added to a cuvette with 210 μM NADH. The change in OD340 was fitted linearly to calculate loss of NADH (6220 $M^{-1}cm^{-1}$ at 340 nm), enabling calculation of k_{cat}. Reactions were repeated 3 times, and the error represents the SD.

DNA substrates

F26,50 (5′-GACTACGTACTGTTACGGCTCCATC[FlcdT]CTACCGCAATCAGGCCAGATCTGC-3′) containing a fluorescein adduct opposite a mismatched base was previously demonstrated as a target for NER (22). Double-stranded substrate was produced by mixing equimolar concentrations of the reverse, complementary nondamaged oligonucleotide in TE buffer [10 mM Tris-HCl, 1 mM EDTA (pH 8)] at 95°C and left to cool slowly to room temperature. Cyclobutane pyrimidine dimers pUC18 and λ DNA (New England Biolabs, Ipswich, MA, USA) were irradiated to 1000 J/m^2 with a calibrated 254 nm lamp (ENF-240C/FE; Spectronics, Westbury, NY, USA) immediately before being used in the ATPase assay.

DNA tightropes

DNA tightropes were constructed as previously described (21). Nucleotides [ATP, ADP, adenosine 5′-O-(3-thio)triphosphate (ATPγS)] were used at 1 mM final concentration. For experiments with P_i, 1 mM ADP with 50 mM Tris-HCl (pH 7.5), 10 mM $MgCl_2$, and 10 mM DTT was supplemented with 19 mM sodium phosphate (freshly autoclaved to remove pyrophosphate), and ionic strength was balanced by the removal of 50 mM KCl (23). For experiments with damaged λ DNA, the DNA was exposed to 1000 J/m^2 of 254 nm light immediately before creating tightropes.

Single molecule imaging and analysis

Imaging was performed using a custom-built fluorescence microscope capable of oblique-angle fluorescence excitation and multichannel emission (21). mScarlet was excited using a 561 nm diode OBIS LS laser (Coherent, Santa Clara, CA, USA) at 5 mW. To determine if photobleaching affected our observed attached lifetimes, we measured durations of attachment for the longest associating nucleotide condition, UvrA-ATPγS, at different laser powers. The attached lifetime was reduced only above 10 mW, indicating that, at the laser powers used in our experiments, photobleaching is not defining the lifetime. Videos were collected with a 300 ms exposure time for 90 s using 2 × 2 binning and were transformed into kymographs using ImageJ.

Attached lifetimes in each condition were plotted as cumulative frequency histograms to remove any bin size dependence. Cumulative frequencies were fitted to exponentials, and F-tests were used to determine the requirement for single *vs.* double exponential fits.

RESULTS

DNA accelerates the steady-state ATP hydrolysis rate of UvrA

Although it is known that *E. coli* nucleotide excision repair requires ATP (3, 6, 7), its role in UvrA's function has not been fully determined. Using an NADH-linked assay, the steady-state UvrA-mScarlet (UvrA hereafter) ATP turnover rate was measured with and without DNA. Absorbance at 340 nm was used to linearly quantify ADP release because

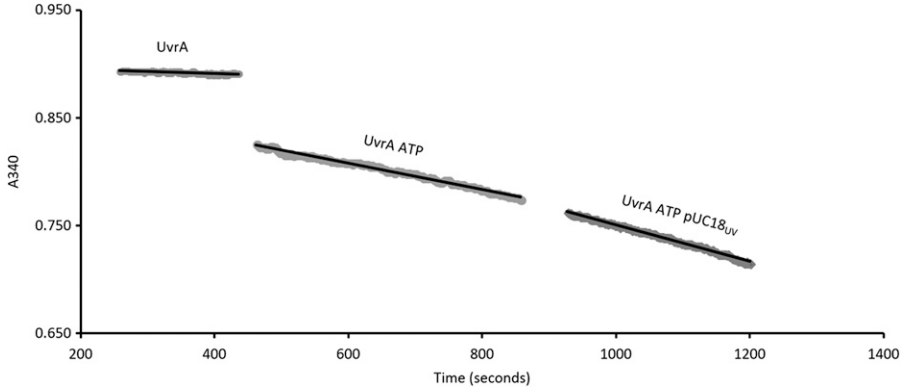

Figure 1. Real-time NADH-coupled ATPase assay. UvrA alone, UvrA with 1 mM ATP added and after the addition of 50 ng 1000 J/m^2 irradiated pUC18. Rates of NAD^+ production include: UvrA, 0.002 μM/s; UvrA + ATP, 0.020 μM/s; and UvrA + ATP + DNA, 0.027 μM/s. Reactions were carried out at room temperature in ABC buffer with 25 nM UvrA-mScarlet; no ADP accumulates in this coupled assay.

1 NADH is oxidized to NAD^+ for each ADP released. Linear fits gave the rates of ATP hydrolysis shown in **Fig. 1**.

This assay was repeated for various damaged and undamaged DNA substrates (**Fig. 2*A***). Undamaged DNA substrates stimulate the ATPase activity of UvrA significantly (k_{cat} UvrA alone, 0.71 ± 0.05 ATP/UvrA/second *vs.* UvrA + undamaged DNA, 1.07 ± 0.08 ATP/UvrA/second; $P < 0.0001$). The ATPase rate was also stimulated by a fluorescein containing oligonucleotide F26,50 (1.06 ± 0.142 ATP/UvrA/second), UV damaged pUC18 (1.13 ± 0.05 ATP/UvrA/second), or λ phage DNA (1.03 ± 0.12 ATP/UvrA/second) compared with ATP alone ($P < 0.0001$). However, damaged DNA does not affect the maximal ATPase activity relative to undamaged equivalents ($P = 0.9594$) (Fig. 2*A*, combined data). To investigate if damage discrimination affects UvrA's ATPase, we titrated ATP (Fig. 2*B*) in the presence of undamaged DNA or UV-irradiated DNA. The K_m for ATP decreased from 195 μM in the presence of undamaged DNA to 60 μM with damaged DNA. The ATP titration independently confirmed that the k_{cat} (per UvrA monomer) was unchanged, remaining at 1.4/s. Because ATP hydrolysis is accelerated by DNA binding, this indicates that the rate-limiting kinetic process occurs while bound to DNA. If the rate-limiting step did not occur on DNA, there would be no change in steady-state ATPase upon addition of DNA.

Determining the kinetic state affected by DNA binding

To identify which nucleotide state is affected by DNA binding, we measured the DNA-bound lifetime of UvrA using single-molecule fluorescence imaging. To do this, we used an *in vitro* DNA tightrope assay, which comprises individual DNA molecules suspended between silica beads in a microfluidic chamber (24, 25). Oblique angle illumination is used to limit the background from molecules in solution, leading to clear images of mScarlet-labeled protein binding to the DNA tightropes. The effects of damage were studied using DNA exposed to UV light (254 nm) immediately before the formation of tightropes. Videos of UvrA molecules binding to DNA were transformed into kymographs (**Fig. 3*A***) for dwell-time analysis and determination of the search mechanism. One-dimensional sliding on DNA will appear as movement on the Y axis (position) over time, whereas a 3-dimensional search will appear as horizontal streaks (24) (Fig. 3*A*). The length of any continuous interaction corresponds to the dwell time. It was clear from the data that UvrA uses a 3-dimensional search mechanism because no positional movement was seen. The individual attached lifetimes were plotted as cumulative frequency histograms and fit to exponentials, which are appropriate for stochastic interactions (Fig. 3*B*). These fits across various nucleotide and DNA damage conditions provided dissociation rate constants (Fig. 3*C* and **Table 1**).

The bulk-phase steady-state ATPase k_{cat} was determined to be 1.07 ATP/UvrA per second in the presence of damaged or undamaged DNA (Fig. 2). This is in excellent agreement with the single-molecule detachment rate constant of 1.24 ± 0.038/s for UvrA on undamaged DNA with ATP. These data fit better to a double exponential (F-test = 204) than a single, suggesting 2 populations of attachments, the vast majority of which (amp1 = 94%) reflect molecules binding to undamaged DNA. The remainder most likely represents molecules that bind to nonspecific damage on λ DNA, as previously shown (24). In the presence of UV-damaged DNA and ATP, UvrA shows a dramatic decrease in the detachment rate constant (0.411 ± 0.023/s; *i.e.*, a 3-fold increase in attached lifetime). The UV damage cumulative frequency histogram also fits better to a double exponential (F-test = 154; amp1 96%, *k*1 0.411 ± 0.023/s; amp2 4%, *k*2 0.098 ± 0.030/s; Fig. 3*B*), consistent with 2 populations of attached proteins. However, the small contribution (amp2 = 4%) of *k*2 means very few complexes are long lived on DNA. We did not investigate the origin of this species further.

To determine the contribution of the ATP binding to the attached lifetime of UvrA, we used ATPγS, a nonhydrolyzable analog of ATP. ATPγS has been shown to permit formation of UvrA dimers and stimulate binding of UvrA to DNA (5). Figure 3*C* shows that ATPγS slows the release of UvrA from DNA (0.155 ± 0.002/s), equivalent to a 6.5-fold increase in attached lifetime. DNA damage does not affect the dissociation kinetics of UvrA in the presence of ATPγS (0.127 ± 0.001/s), suggesting that ATP-bound UvrA is not involved in damage recognition (5, 12). The slow rate constant for ATP-bound detachment implies that hydrolysis and formation of subsequent nucleotide states occur on DNA; consequently, one of these states will be sensitive to damage.

A possible candidate for controlling the release of UvrA from DNA is the ADP-bound state. ADP facilitates UvrA

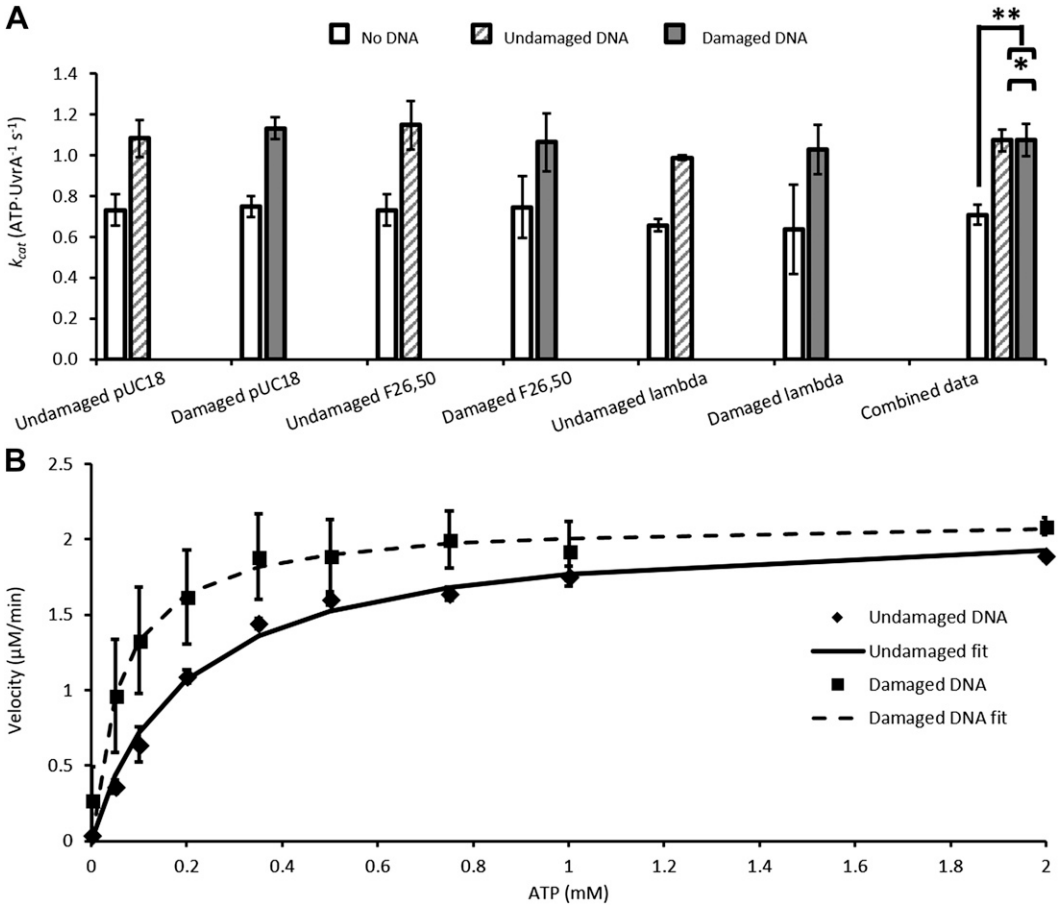

Figure 2. Steady-state ATPase data for UvrA. *A*) Summary of the k_{cat} per UvrA monomer for no DNA (white), undamaged DNA (striped gray), and 1000 J/m^2 UV-damaged DNA (solid gray). All data were collected using the linked assay (Fig. 1). Error bars are SD for 3 repeat determinations. Combined data were obtained from the mean of all non-DNA, undamaged DNA, and damaged DNA ATPase rates. Combined data show that damaged DNA (1.074 ATP/UvrA per second) does not differ from undamaged DNA (1.073 ATP/UvrA per second). *P = 0.9594, **$P < 0.0001$ (Student's t test). *B*) ATP titration of UvrA ATPase with undamaged or UV damaged DNA. In the presence of damage (squares), the K_m is decreased 3-fold compared with undamaged DNA (diamonds). The k_{cat} is unchanged between conditions. Data are averages of 3 repeats, and error is SD.

dimerization and binding to DNA (4, 11, 12). Surprisingly, UvrA in the presence of ADP did not substantially bind to DNA tightropes compared with identical concentrations of UvrA with ATP or ATPγS. Nonetheless, from the attachments observed it was possible to determine the lifetime as 4.9 s (0.20 ± 0.006/s), which was ~5-fold longer than in the presence of ATP. The low level of attachment suggests that few UvrA dimers exist in the presence of ADP (5), conflicting with previous observations (12). With UV-damaged DNA, the attached lifetime remains unchanged at 4.6 s (equivalent to 0.22 ± 0.016/s). It is likely that UvrA does not dimerize with only ADP bound and that the few dimers that form are strongly bound to the DNA. Given the low abundance of this state, it is likely that detachment occurs from the ADP state. Furthermore, the similar rates of release in the presence and absence of DNA damage suggest that UvrA-ADP is not a damage sensing state.

The step between ATP binding and formation of the UvrA ADP-bound state is therefore the most likely to detect damage. To investigate this, we attempted to create the ADP.P_i state of UvrA by adding a large excess of free phosphate to UvrA and ADP. This required careful consideration of ionic strength changes that were balanced by a reduction in the buffer salt (26). On undamaged DNA, the addition of phosphate to the ADP state increases the detachment rate constant slightly from ADP alone (0.202 ± 0.006 to 0.234 ± 0.007/s) but does not resemble the ATP condition (1.07 ± 0.019/s), nor does phosphate restore UvrA's affinity for DNA; the number of binding events was also low, similar to the ADP-bound state. It is clear that P_i addition does not reverse hydrolysis and restore the rate-limiting step for detachment. However, in the presence of UV-damaged DNA, UvrA's detachment rate constant significantly increases (from 0.217 ± 0.016 to 0.364 ± 0.011/s; $P < 0.0001$), resembling the rate constant for release in the presence of UV damage and ATP (0.411 ± 0.023/s; P = 0.501). This change in lifetime suggests that UvrA with P_i and ADP is populating the damage-sensitive state, which is rate limiting for UvrA detachment from DNA.

DISCUSSION

The role of ATP in the mechanism of NER is not clearly understood. Here, we compare the kinetics of ATP turnover by UvrA at the bulk- and single-molecule level. We

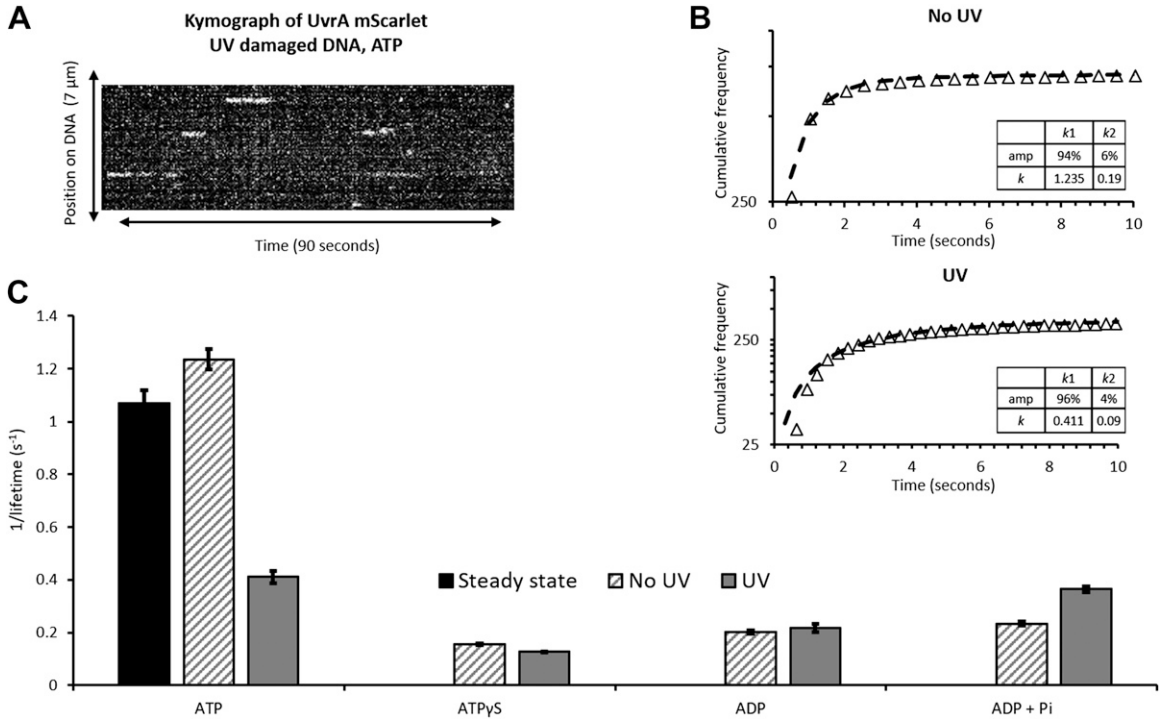

Figure 3. The single-molecule binding kinetics of UvrA. *A*) A kymograph transformation from a video showing UvrA-mScarlet binding and releasing from DNA in a 3-dimensional search. *B*) Lengths of the linear streaks in *A* were compiled into cumulative frequency histograms. The data for UvrA with ATP and DNA, either undamaged (top) or UV irradiated (bottom), are shown as logarithmic cumulative frequency against time; the nonlinearity indicates 2 processes. These were fit to double exponentials with rate constants given in the inset. *C*) A comparison of the rate constants obtained for each nucleotide and DNA condition (Table 1). The steady-state k_{cat} (Fig. 2) is shown as a solid black bar. Error bars indicate the SEM fit error.

have found that the bulk-phase ATPase k_{cat} of UvrA was stimulated by the presence of DNA; however, there was no further change with damaged DNA. This strongly contrasted with the attached lifetimes of UvrA on DNA. The presence of damage increased the attached lifetime 2- to 3-fold in the presence of ATP. After determining the attached lifetimes of UvrA molecules on either damaged or undamaged DNA under various nucleotide conditions, we infer that UvrA most likely functions as a negatively cooperative ATPase, using its 2 ATP sites in sequence.

TABLE 1. *Summary of rate constants for various nucleotide conditions on undamaged or UV-damaged DNA*

Nucleotide	Detachment rate constant per second	Fit error	*N*
No damage			
ATP	1.235[a]	0.038	706
ATPγS	0.155	0.002	166
ADP	0.202	0.006	33
ADP Pi	0.234	0.007	53
UV damage			
ATP	0.411[b]	0.023	394
ATPγS	0.127	0.001	152
ADP	0.217	0.016	21
ADP Pi	0.364	0.011	43

N refers to molecules analyzed from at least 3 flow cells per condition. [a]Double exponential, amp1 94%, *k*1 1.235 ± 0.038 s^{-1}; amp2 6%, *k*2 0.190 ± 0.044 s^{-1}. [b]Double exponential, amp1 96%, *k*1 0.411 ± 0.023 s^{-1}; amp2 4%, *k*2 0.098 ± 0.030 s^{-1}.

UvrA's second ATPase site is activated by DNA damage

The steady-state ATPase rate for UvrA increased ~50% upon addition of DNA, demonstrating that UvrA is a DNA-stimulated ATPase. However, no further change in the DNA-stimulated ATPase was observed with damaged DNA. Similar changes in bulk-phase ATPase using the linked assay have been reported (17). We used damage substrates at various damage densities and different types of substrate (see Supplemental Information); however, in all conditions the type or density of damage had no effect on the observed results. We also ensured the DNA damage concentration was higher than the UvrA concentration used. Furthermore, linear and plasmid DNA substrates stimulated the ATPase of UvrA equally, indicating that the DNA ends play no part in the observed activation. This contrasts with previous studies, where undamaged DNA was seen to inhibit the ATPase and damage returned the activity to that seen without DNA (16). This difference may be due to ADP's strong affinity for UvrA (14), which may inhibit the ATPase; our use of the linked assay ensures nucleotide is recycled, abrogating any possible issues arising from such product inhibition.

By directly imaging single UvrA molecules binding to DNA, we were able to correlate attached lifetimes with the biochemically measured ATPase rates. With ATPγS, ample binding to DNA was observed; however, with ADP this was virtually abolished, suggesting that UvrA binds DNA

in the ATP-bound state and releases from DNA in the ADP-bound state. In both cases the attached lifetimes are too long to correlate with the steady-state ATPase rate and were not affected by DNA damage; therefore, these states are unlikely to be substantially populated, and their role in the damage-modulated ATPase of UvrA is irrelevant. The most interesting observation derives from a comparison of the bulk k_{cat} of 1/s *vs.* the lifetime in the presence of ATP (~1/s); these values are identical. The k_{cat} was calculated per UvrA monomer; therefore, we infer that on DNA where UvrA is a dimer (4, 12, 24, 27) 2 ATP molecules are hydrolyzed and that attachment to DNA is tightly coupled to ATP turnover. However, in the presence of damage, although k_{cat} is unchanged, the attached lifetime increases substantially. The ~3-fold increased affinity for ATP on damaged DNA corresponds well to the 3-fold increase in lifetime on damaged DNA, demonstrating that, in the presence of damage, there remains tight coupling between ATP turnover and UvrA release from DNA. Therefore, to reconcile the unchanged k_{cat} with the increased lifetime, we suggest that when damage is detected during turnover of the first ATP, rather than detaching from DNA, the second site is activated. This second site has a similar ATP hydrolysis rate, thus keeping the total number of ATPs hydrolyzed per second the same but increasing the attached lifetime. This sequential action is indicative of negative cooperativity between the sites that is tightly coupled to DNA damage recognition. Similar mechanisms of negative cooperativity have been noted for other ABC ATPase superfamily members, including the bacterial mismatch repair protein MutS (28) and its eukaryotic homolog (29, 30).

UvrA's rate-limiting step is affected by the presence of DNA damage

Because the rate-limiting step is not ADP release, we sought to determine whether hydrolysis and subsequent release of P_i controls the turnover rate. To push the pathway backward, P_i was added to ADP and UvrA. If ATP hydrolysis and release of ADP + P_i is the rate-limiting step, the addition of P_i to ADP should restore the lifetime to the ATP condition. With undamaged DNA, the detachment rate constant did not resemble that of UvrA in the presence of ATP (0.23 *vs.* 1.2/s). Therefore, the addition of phosphate does not reverse hydrolysis of the first site. However, with damaged DNA the detachment rate constant was very similar to that of UvrA with ATP and UV damage (0.36 *vs.* 0.41/s). We surmised that the 0.41/s detachment rate constant was derived from sequential ATP hydrolysis at both sites. This suggests that, in the presence of damage, both nucleotide binding sites can reload P_i and that the rate-limiting steps are recapitulated, possibly through reversal of hydrolysis. The identity of the 2 sites was revealed using ATPase mutants (14) and *in vivo* (13). Based on these previous observations that nucleotide needs to be bound to the C-terminal (or distal) ATPase site for damage recognition, we suggest this is the first ATPase site described here. Therefore, the second ATPase site (N-terminal or proximal) is activated after damage recognition at the first site. This confirms the 2-site hypothesis, which suggests the N-terminal site is necessary for recruitment of UvrB (13, 14, 17).

Communication between the ATPase sites is likely facilitated by their close proximity. The N-terminal site of 1 ATPase site is adjacent to the C-terminal site. Interestingly, these sites are connected by a tunnel (**Fig. 4**); it is plausible that P_i release occurs through this tunnel and gates the recruitment of nucleotide or hydrolysis at the second site. Future structural investigations of the transition state are imperative to reveal how P_i is released, whether through the tunnel or by monomerization.

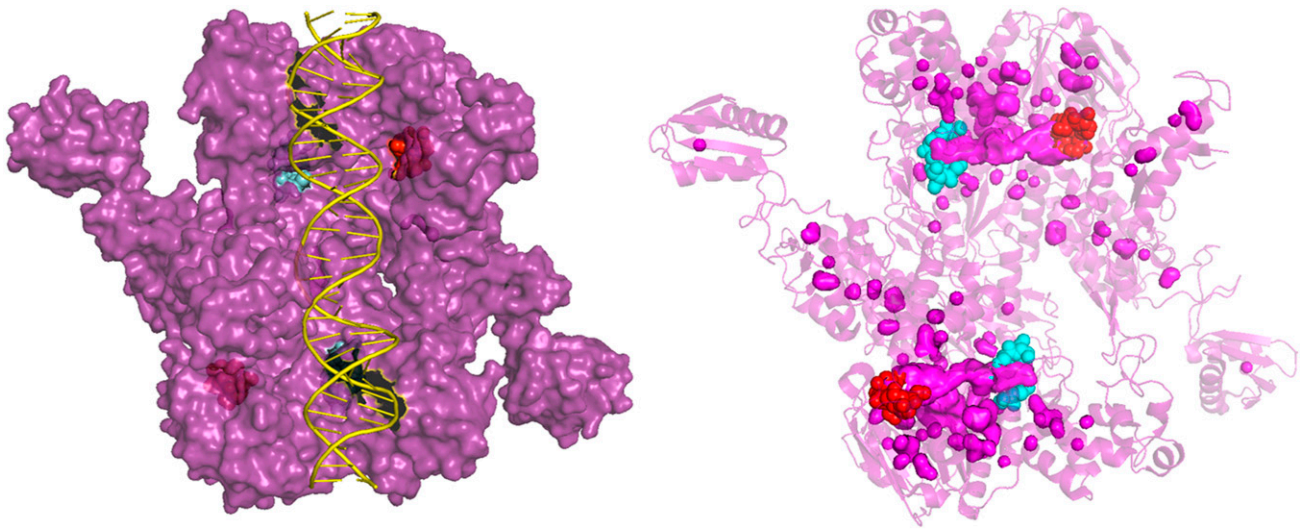

Figure 4. Crystal structure of *Thermotoga maritima* UvrA showing the phosphate tunnel. Left: Surface plot of dimeric UvrA (purple) with the N-terminal (cyan) and C-terminal (red) ATPase sites shown behind DNA (yellow) forming a tunnel. Right: PyMol cavity search of structure revealing a clear tunnel (pink) with the ATPase sites (cyan and red) on either side. UvrA is shown as a transparent cartoon with all pink surface objects showing solvent cavities. Image created in PyMol using PDB structure (3PIH) (9).

CONCLUSIONS

In summary, we have combined data from single-molecule and bulk-phase studies of the UvrA ATPase and DNA interaction. We find excellent correlation between the kinetics using both methods and that UvrA's interaction with DNA is tightly coupled to its ATPase rate-limiting step. Two ATPs are hydrolyzed per dimer per second when bound to undamaged DNA. However, in the presence of damage, although the steady-state ATPase is unaltered, the attached lifetime increases. We suggest this occurs through a sequential mechanism whereby if damage is located, the second ATPase site is activated, resulting in another 2 ATPs per dimer per second being hydrolyzed. This accounts for the observed kinetics and suggests a tight coupling model due to strong negative cooperativity between the UvrA ATPase sites. Therefore, UvrA couples its ATPase activity to its damage-sensing function by activating the second ATPase site. FJ

ACKNOWLEDGMENTS

The authors thank the Kad group for discussion; Bennett Van Houten, (University of Pittsburgh, Pittsburgh, PA, USA) Chris Mulligan, Alex Moores, and Michael Geeves (all of the University of Kent) for reading the manuscript; the National Institute of Genetics, Japan for access to their excellent collection of materials; and Alex Moores for constructing the empty mScarlet vector used in this study. This work was supported by Biotechnology and Biological Sciences Research Council Grants BB/P00847X/1, BB/M019144/1, and BB/I003460/1 (to N.M.K.) and BB/M01603X/1 (to J.T.B.). The authors declare no conflicts of interest.

AUTHOR CONTRIBUTIONS

J. T. Barnett collected data; and J. T. Barnett and N. M. Kad designed the experiments, analyzed the data, and wrote the manuscript.

REFERENCES

1. Truglio, J. J., Croteau, D. L., Van Houten, B., and Kisker, C. (2006) Prokaryotic nucleotide excision repair: the UvrABC system. *Chem. Rev.* **106**, 233–252
2. Van Houten, B., Croteau, D. L., DellaVecchia, M. J., Wang, H., and Kisker, C. (2005) 'Close-fitting sleeves': DNA damage recognition by the UvrABC nuclease system. *Mutat. Res.* **577**, 92–117
3. Sancar, A., and Rupp, W. D. (1983) A novel repair enzyme: UVRABC excision nuclease of Escherichia coli cuts a DNA strand on both sides of the damaged region. *Cell* **33**, 249–260
4. Orren, D. K., and Sancar, A. (1989) The (A)BC excinuclease of Escherichia coli has only the UvrB and UvrC subunits in the incision complex. *Proc. Natl. Acad. Sci. USA* **86**, 5237–5241
5. Seeberg, E., and Steinum, A. L. (1982) Purification and properties of the uvrA protein from Escherichia coli. *Proc. Natl. Acad. Sci. USA* **79**, 988–992
6. Yeung, A. T., Mattes, W. B., Oh, E. Y., and Grossman, L. (1983) Enzymatic properties of purified Escherichia coli uvrABC proteins. *Proc. Natl. Acad. Sci. USA* **80**, 6157–6161
7. Thiagalingam, S., and Grossman, L. (1991) Both ATPase sites of Escherichia coli UvrA have functional roles in nucleotide excision repair. *J. Biol. Chem.* **266**, 11395–11403
8. Husain, I., Van Houten, B., Thomas, D. C., and Sancar, A. (1986) Sequences of Escherichia coli uvrA gene and protein reveal two potential ATP binding sites. *J. Biol. Chem.* **261**, 4895–4901
9. Jaciuk, M., Nowak, E., Skowronek, K., Tańska, A., and Nowotny, M. (2011) Structure of UvrA nucleotide excision repair protein in complex with modified DNA. *Nat. Struct. Mol. Biol.* **18**, 191–197
10. Pakotiprapha, D., Inuzuka, Y., Bowman, B. R., Moolenaar, G. F., Goosen, N., Jeruzalmi, D., and Verdine, G. L. (2008) Crystal structure of Bacillus stearothermophilus UvrA provides insight into ATP-modulated dimerization, UvrB interaction, and DNA binding. *Mol. Cell* **29**, 122–133
11. Oh, E. Y., Claassen, L., Thiagalingam, S., Mazur, S., and Grossman, L. (1989) ATPase activity of the UvrA and UvrAB protein complexes of the Escherichia coli UvrABC endonuclease. *Nucleic Acids Res.* **17**, 4145–4159
12. Mazur, S. J., and Grossman, L. (1991) Dimerization of Escherichia coli UvrA and its binding to undamaged and ultraviolet light damaged DNA. *Biochemistry* **30**, 4432–4443
13. Stracy, M., Jaciuk, M., Uphoff, S., Kapanidis, A. N., Nowotny, M., Sherratt, D. J., and Zawadzki, P. (2016) Single-molecule imaging of UvrA and UvrB recruitment to DNA lesions in living Escherichia coli. *Nat. Commun.* **7**, 12568
14. Myles, G. M., Hearst, J. E., and Sancar, A. (1991) Site-specific mutagenesis of conserved residues within Walker A and B sequences of Escherichia coli UvrA protein. *Biochemistry* **30**, 3824–3834
15. Myles, G. M., and Sancar, A. (1991) Isolation and characterization of functional domains of UvrA. *Biochemistry* **30**, 3834–3840
16. Wagner, K., Moolenaar, G. F., and Goosen, N. (2010) Role of the two ATPase domains of Escherichia coli UvrA in binding non-bulky DNA lesions and interaction with UvrB. *DNA Repair (Amst.)* **9**, 1176–1186
17. Kraithong, T., Channgam, K., Itsathitphaisarn, O., Tiensuwan, M., Jeruzalmi, D., and Pakotiprapha, D. (2017) Movement of the β-hairpin in the third zinc-binding module of UvrA is required for DNA damage recognition. *DNA Repair (Amst.)* **51**, 60–69
18. Croteau, D. L., DellaVecchia, M. J., Wang, H., Bienstock, R. J., Melton, M. A., and Van Houten, B. (2006) The C-terminal zinc finger of UvrA does not bind DNA directly but regulates damage-specific DNA binding. *J. Biol. Chem.* **281**, 26370–26381
19. Bindels, D. S., Haarbosch, L., van Weeren, L., Postma, M., Wiese, K. E., Mastop, M., Aumonier, S., Gotthard, G., Royant, A., Hink, M. A., and Gadella, T. W., Jr. (2017) mScarlet: a bright monomeric red fluorescent protein for cellular imaging. *Nat. Methods* **14**, 53–56
20. Kitagawa, M., Ara, T., Arifuzzaman, M., Ioka-Nakamichi, T., Inamoto, E., Toyonaga, H., and Mori, H. (2005) Complete set of ORF clones of Escherichia coli ASKA library (a complete set of E. coli K-12 ORF archive): unique resources for biological research. *DNA Res.* **12**, 291–299
21. Springgall, L., Hughes, C. D., Simons, M., Azinas, S., Van Houten, B., and Kad, N. M. (2018) Recruitment of UvrBC complexes to UV-induced damage in the absence of UvrA increases cell survival. *Nucleic Acids Res.* **46**, 1256–1265
22. DellaVecchia, M. J., Croteau, D. L., Skorvaga, M., Dezhurov, S. V., Lavrik, O. I., and Van Houten, B. (2004) Analyzing the handoff of DNA from UvrA to UvrB utilizing DNA-protein photoaffinity labeling. *J. Biol. Chem.* **279**, 45245–45256
23. Bers, D. M., Patton, C. W., and Nuccitelli, R. (2010) A practical guide to the preparation of Ca(2+) buffers. *Methods Cell Biol.* **99**, 1–26
24. Kad, N. M., Wang, H., Kennedy, G. G., Warshaw, D. M., and Van Houten, B. (2010) Collaborative dynamic DNA scanning by nucleotide excision repair proteins investigated by single- molecule imaging of quantum-dot-labeled proteins. *Mol. Cell* **37**, 702–713
25. Springgall, L., Inchingolo, A. V., and Kad, N. M. (2016) DNA-protein interactions studied directly using single molecule fluorescence imaging of quantum dot tagged proteins moving on DNA tightropes. *Methods Mol. Biol.* **1431**, 141–150
26. Kad, N. M., Trybus, K. M., and Warshaw, D. M. (2008) Load and Pi control flux through the branched kinetic cycle of myosin V. *J. Biol. Chem.* **283**, 17477–17484
27. Malta, E., Moolenaar, G. F., and Goosen, N. (2007) Dynamics of the UvrABC nucleotide excision repair proteins analyzed by fluorescence resonance energy transfer. *Biochemistry* **46**, 9080–9088
28. Lamers, M. H., Winterwerp, H. H., and Sixma, T. K. (2003) The alternating ATPase domains of MutS control DNA mismatch repair. *EMBO J.* **22**, 746–756
29. Iaccarino, I., Marra, G., Palombo, F., and Jiricny, J. (1998) hMSH2 and hMSH6 play distinct roles in mismatch binding and contribute differently to the ATPase activity of hMutSalpha. *EMBO J.* **17**, 2677–2686
30. Studamire, B., Quach, T., and Alani, E. (1998) Saccharomyces cerevisiae Msh2p and Msh6p ATPase activities are both required during mismatch repair. *Mol. Cell. Biol.* **18**, 7590–7601

Received for publication May 8, 2018.
Accepted for publication July 2, 2018.